Inter-individual differences in T1, T2, and proton density using quantitative synthetic imaging for 1H-MRS quantification

Magnetic Resonance in Medicine

WILEY | ISMRM ONE COMMUNITY FOR CLINICIANS AND SCIENTISTS

RESEARCH ARTICLE OPEN ACCESS

Inter-Individual Differences in T_1, T_2, and Proton Density Using Quantitative Synthetic Imaging for ^{1}H-MRS Quantification

Samantha A. Leech[1,2,3,4] | Sarah L. Manske[2] | Paul G. Mullins[5] | Tiffany K. Bell[2,3,4,6] | Ashley D. Harris[2,3,4]

[1]Department of Biomedical Engineering, Schulich School of Engineering, University of Calgary, Calgary, Alberta, Canada | [2]Department of Radiology, Cumming School of Medicine, University of Calgary, Calgary, Alberta, Canada | [3]Hotchkiss Brain Institute, Cumming School of Medicine, University of Calgary, Calgary, Alberta, Canada | [4]Alberta Children's Hospital Research Institute, University of Calgary, Calgary, Alberta, Canada | [5]Bangor Imaging Center, School of Psychology and Sports Science, Bangor University, Bangor, Gwynedd, UK | [6]School of Psychology and Clinical Language Sciences, University of Reading, Reading, UK

Correspondence: Tiffany K. Bell (t.bell@reading.ac.uk)

Received: 20 August 2025 | **Revised:** 10 December 2025 | **Accepted:** 30 December 2025

ABSTRACT

Purpose: Metabolite concentrations can be determined from proton magnetic resonance spectroscopy (^{1}H-MRS) data using water as an internal reference. This calculation requires tissue-specific water T_1 and T_2 relaxation constants and proton density (PD). Although literature values are commonly used, these vary with age and within clinical conditions, potentially introducing variability or masking metabolite effects. The introduction of rapid multi-dynamic multi-echo (MDME) imaging to generate multiparametric maps allows fast measurement of these parameters for each individual within a single acquisition.

Methods: ^{1}H-MRS and MDME data were collected from 26 healthy volunteers (aged 18–40 years). The agreement between metabolite concentrations derived using individually measured T_1, T_2 and PD values and literature-based values was assessed. A sensitivity analysis was also used to determine the impact of extended value ranges on metabolite concentrations.

Results: Using a MDME sequence to determine individually measured T_1, T_2, and PD values for tissue correction was successful. Strong agreement between metabolite concentrations calculated using literature and measured values was seen, although concentrations calculated using literature values tended to be slightly higher than when using measured values. The sensitivity analysis showed T_1 relaxation contributed most strongly to the calculated concentration variability.

Conclusion: This study demonstrates the feasibility of using a MDME acquisition to acquire individual- specific parameter values for tissue correction. This provides a fast, effective method to acquire individual relaxation parameters, which will be highly relevant for populations where these parameters will vary (such as the elderly, pediatrics or with clinical diagnoses).

1 | Introduction

Proton magnetic resonance spectroscopy (^{1}H-MRS) measures a neurochemical signal over a region of interest (voxel). The conversion of this signal into a concentration (usually in moles per kg or moles per liter) requires comparison of the neurochemical signal with tissue water signal. This necessitates knowledge of T_1 and T_2 relaxation times and proton density (PD), as the signals are not typically in a fully relaxed condition [1]. Large voxel sizes are needed due to the low neurochemical signal intensity, and

Tiffany K. Bell and Ashley D. Harris contributed equally to this work.

therefore will encompass a mixture of gray matter (GM), white matter (WM), and cerebrospinal fluid (CSF). Therefore, knowledge of the relaxation times and PD of the different tissue types is required.

Relaxation times and PD are generally obtained from the literature, with a single value often measured from healthy young adults used as a representative value [1]. This relies on the assumption that these values do not vary significantly between individuals or brain regions. However, there is variation in the reported values of T_1, T_2, and PD, likely due to differences in location of the measurement in the brain and the technique used [2, 3]. Therefore, a range of values are often used across ^{1}H-MRS studies, and calculated concentrations will differ between studies depending on the source of the relaxation factors used. Additionally, T_1, T_2, and PD have been shown to vary non-linearly with age [4–9], and are altered in clinical conditions [10–13]. These variations can potentially lead to erroneous conclusions, for example a change in neurochemical concentration across age could be driven or masked by a change in T_1, T_2 or PD. Indeed, Sporn et al. used ^{1}H-MRS with a long TR to reduce T_1 effects, and found-age related changes in hippocampal metabolites that were not seen in previous studies using a short TR, where T_1 weighting will impact metabolite levels [14]. However, the use of a long TR does not address T_2 effects, and may not be appropriate in populations that are unable to remain still in the scanner and will require downweighing of several transients.

A more accurate approach would be to explicitly measure these constants in the spectroscopy voxel [15]. However, this previously required the use of multiple sequences, some of which are not routinely provided by vendors. This would prohibitively increase scan time and may not be accessible for a clinical routine protocol. More recently, multi-dynamic multi-eco (MDME) acquisitions have been developed such that these parameters can be quantified within a single acquisition, mitigating the time burden associated with their measurement [16]. This sequence optimizes time efficiency by reading previously encoded slices to eliminate the waiting periods following saturation pulses [17–19]. Quantitative maps for T_1, T_2, and PD can then be generated [20]. A voxel mask can then be used to measure region specific values from the same area the neurochemical signal was acquired. Although tissue specific values are typically used, this method allows an average measurement of T_1, T_2, and PD over the whole voxel. This is a simpler approach and removes the potential for errors caused by tissue segmentation which can propagate to the end concentration value.

This study aimed to address the feasibility of using a MDME acquisition to acquire individually measured T_1, T_2, and PD values for calculating neurochemical concentrations. Additionally, we assessed the effect of using individually measured parameters on neurochemical concentration compared to using values obtained from the literature (denoted as LIT). We measured values from the full voxel (denoted as FULL), as well as tissue segmented values (denoted as SEG). Further, we used a sensitivity analysis to assess the overall impact of varying ranges of T_1, T_2, and PD on concentration measures using ranges obtained from our sample, as well as a larger range obtained from the literature to encompass variation seen across a broader age range and clinical conditions.

2 | Methods

2.1 | Participants

Data were collected from 26 participants (aged 18–40 years, 18 female). Participants were in good health and free from contraindications to MRI. Ethics approval was obtained from the Conjoint Health Research Ethics Board at the University of Calgary (REB22-0738), and all participants provided written informed consent upon enrollment.

2.2 | Data Acquisition

Data were collected at 3 T (GE 750 W) using a 32-channel head coil. First, a standard T_1-weighted structural image was acquired (TR/TE = 7.4/2.7 ms and 1 mm^3 isotropic voxels) for voxel placement and tissue segmentation. ^{1}H-MRS data were collected in six voxels, as shown in Figure 1. Voxels were placed to encompass a variety of tissue compositions, with the goal of defining primarily WM, primarily GM, and mixed WM and GM in anterior and posterior regions of the brain. Semi-Localization by Adiabatic SElective Refocusing (sLASER) was used to collect ^{1}H-MRS data (TR/TE = 3000/35 ms, voxel size $20 \times 20 \times 20$ mm^3, 96 averages, and VAPOR water suppression) as well as unsuppressed water data for quantification.

Multi-dynamic multi echo (MDME) data were acquired using a 3D MAGnetic resonance image Compilation, (3D-MAGiC) acquisition (axial acquisition; TR/TE/TI, 7.2/2.8/100 ms; FOV = 24 cm^2; matrix size = 256×256; slice thickness = 1.4 mm; flip angle = 4°; bandwidth = 244.14 Hz/pixel; acquisition time = 4 min 38 s). Phased array uniformity enhancement (PURE) was used to correct for non-uniform receiver coil profiles and auto-calibrating reconstruction for Cartesian imaging (ARC) was used with phase = 2.0 and slice = 1.0. HyperSENSE acceleration with a factor of 1.5 was applied. Quantitative synthetic T_1, T_2, and PD maps were generated using SyMRI using the standardized procedure (prototype 23Q2, v0.45.39) [21]. The theory of generating T_1, T_2, and PD maps from MDME data is outlined in Warntjes et al. [18].

2.3 | ^{1}H-MRS Data Fitting

^{1}H-MRS data were preprocessed using FID-A [22], which included coil combination, elimination of poor-quality averages, frequency drift correction, and zero-order phase correction. Data were eddy current corrected and fit using LCModel 6.3 [23]. A basis set including 23 metabolites was simulated using FID-A with exact timings and RF pulses, and included the following neurochemicals: alanine, aspartate, choline, glycerophosphocholine, phosphocholine, creatine, phosphocreatine, GABA, glutamate, glutamine, lactate, inositol, N-acetylaspartate, N-acetylaspartylglutamate, scyllo-inositol, glutathione, glucose, taurine, β-hydroxybutyrate, citrate, ethanol, glycine, and phosphoethanolamine. Additionally, LCModel default macromolecule basis sets were included. The correction factor of ATT_{H2O} was set to 1 to remove this correction, allowing for manual correction during calculation of concentration. Spectra were excluded if they had a FWHM > 0.07 ppm.

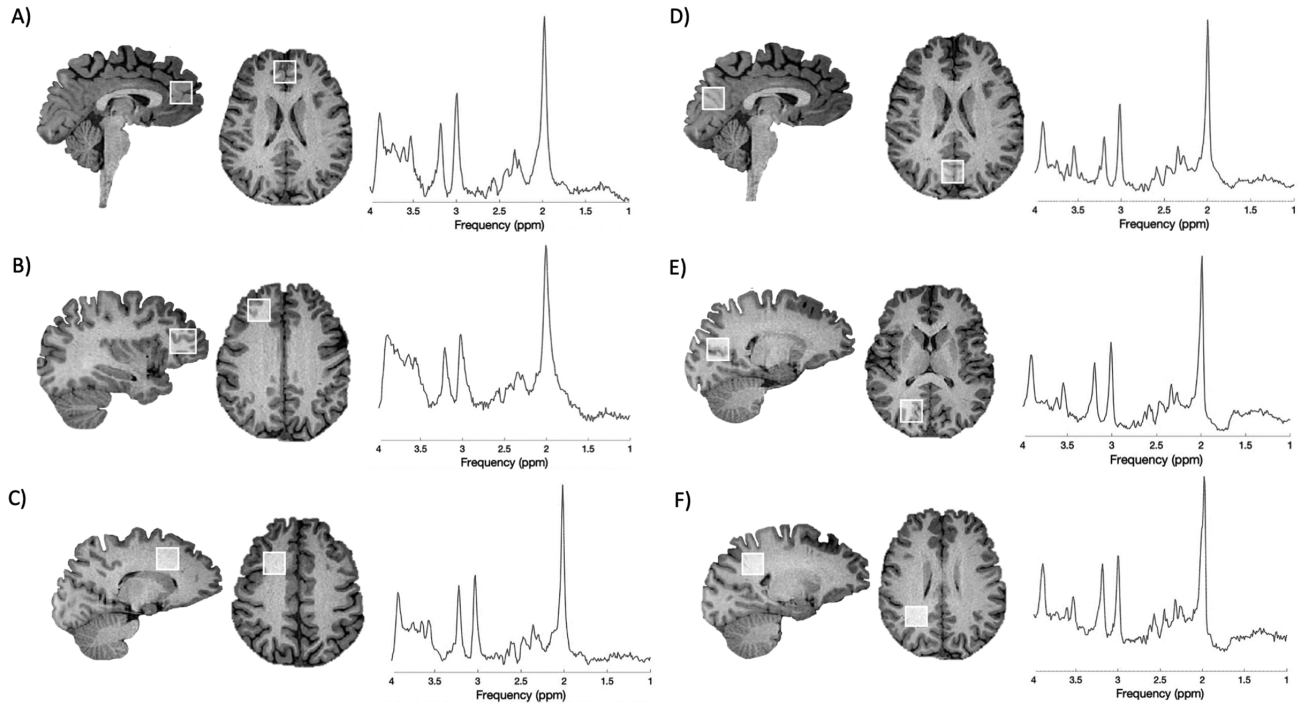

FIGURE 1 | Example placement of the six $2 \times 2 \times 2$ cm^3 voxels with corresponding example spectra. (A) Anterior gray mater, (B) anterior mixed, (C) anterior white matter, (D) posterior gray matter, (E) posterior mixed, and (F) posterior white matter.

2.4 | Quantification

^{1}H-MRS voxel masks were generated and the T_1-weighted structural image segmented into WM, GM, and CSF using the "CoRegStandAlone" co-registration function in Gannet 3.3.1 [24]. These masks were then registered to the T_1, T_2, and PD maps using FSL FLIRT [25], and the voxel average T_1, T_2, and PD values from each voxel mask as well as for WM, GM, and CSF within the voxel were extracted.

Metabolites were quantified as molar concentrations as consensus recommended [1] in three ways. First, data were quantified using literature values for T_1, T_2 and PD in GM, WM and CSF as is standard practice (denoted as LIT). Second, data were quantified using the individualized T_1, T_2, and PD values measured from the whole voxel (not tissue segmented) from each individual's MAGiC acquisition (denoted as FULL) using a modified version of the consensus recommended equation shown below. Third, data were quantified using individualized tissue segmented specific T_1, T_2, and PD values obtained from each individual's MAGiC acquisition (denoted as SEG).

$$[M]_{molar} = C_{raw} \frac{PD_{full} \times R_{H2OFull}}{\left(1 - f_{CSF_{vol}}\right) \times R_{Met}}$$

where $[M]_{molar}$ is the molar concentration of the metabolite, C_{raw} is the moles of metabolite over the moles of water, which is obtained as the MR signal of metabolite over the MR signal of water multiplied by the concentration of water (55.51 mol/kg), $f_{CSF_{vol}}$ is the fraction of CSF in the voxel and PD_{full} is the proton density obtained from the MAGiC acquisition inside the full voxel mask. $R_{H2Ofull}$ is the attenuation factor for water, described as:

$$R_{H2Ofull} = e^{\frac{-TE}{T_{2full}}} \times \left(1 - e^{\frac{-TR}{T_{1full}}}\right)$$

where $T_{1_{full}}$ and $T_{2_{full}}$ are the T_1 and T_2 values obtained from the voxel mask. R_M is the attenuation factor for the metabolite signal, and is described as:

$$R_{Met} = \frac{f_{GM_{vol}} PD_{GM} R_{Met\_GM} + f_{WM_{vol}} PD_{WM} R_{Met\_WM}}{f_{GM_{vol}} PD_{GM} + f_{WM_{vol}} PD_{WM}}$$

where $f_{X_{vol}}$ is the fraction of tissue in the voxel (with x representing GM or WM), PD_x is the proton density within that tissue fraction, and R_{Met_x} is the attenuation factor for each tissue, described as:

$$R_{MetGM} = e^{\frac{-TE}{T_{2metGM}}} \times \left(1 - e^{\frac{-TR}{T_{1}metGM}}\right)$$

$$R_{MetWM} = e^{\frac{-TE}{T_{2metWM}}} \times \left(1 - e^{\frac{-TR}{T_{1}metWM}}\right)$$

Although the relaxation factors from the full voxel were used to avoid errors from segmentation, it is still necessary to use PD values from the individual tissues when calculating R_{Met} to account for the different metabolite relaxation times in GM and WM, as this cannot be measured using the quantitative synthetic maps. See Supporting Information for the metabolite relaxation values used for each tissue.

2.5 | Statistical Analysis

Statistical analyses were performed using RStudio (v2021.09.1 + 372) [26] and Python (v3.13.1, Python Software Foundation, https://www.python.org/). The results from all voxels were

pooled together for analyses. To test for effects of region (anterior/posterior), age and sex on the measured values (T_1, T_2, and PD) while accounting for repeated measures, linear mixed models were conducted using the "lme4" package [27] with subject included as a random effect.

Metabolite concentrations calculated with the different factors were compared using linear mixed models with subject as a random effect, and Bland–Altman plots. The following comparisons were conducted: (1) levels calculated using literature values versus full voxel individual values (LIT vs. FULL) and (2) levels calculated using literature values versus segmented individual values (LIT vs. SEG).

To assess the overall impact of varying ranges of T_1, T_2, and PD on concentration measures, a Sobol sensitivity analysis [28] was conducted in Python. This sensitivity analysis varied all continuous input parameters simultaneously over the entire parameter space to evaluate the relative contributions of each individual parameter, as well as the interactions between parameters, to the model output variance. The model evaluated was the neurochemical concentration of tNAA based on the aforementioned tissue correction model [1, 29] with fixed input parameters for TE = 0.035 s, TR = 3 s, and the T_1 and T_2 values of tNAA in GM and WM (see Supporting Information for the values used). Continuous input parameters to the sensitivity analysis included: water T_1, T_2, and PD, volume fractions of GM, WM, and CSF, and c_{raw} (raw water-referenced signal measure for tNAA). T_1, T_2, and PD were varied within the ranges measured from the quantitative synthetic maps across subjects, while c_{raw} was varied based on the range of non-tissue corrected tNAA levels across subjects. A total of 8192 model evaluations were performed using Saltelli's method [28]. Sensitivity indices greater than 0.05 were interpreted to significantly contribute to the model [28].

Two sensitivity analyses were performed to determine the variance contributions to absolute neurochemical concentrations. These analyses were:

1. Input ranges for T_1, T_2, and PD based on our observed metrics for all six voxels for (a) the full voxel values and (b) the segmented values.
2. Larger input ranges for T_1, T_2, and PD determined by extracting the minimum and maximum values from the literature, to more accurately represent the range in the human brain seen across ages 18–80, and inclusive of clinical conditions. This was also conducted for (a) the full voxel values and (b) the segmented values using the following ranges:
   - T_1 range of 0.6–6.873 s determined from a study investigating age related changes in relaxation times across the ages 20–80 [5] and a review on T_1 relaxation times reported in a systematic compilation of published values [2], as well as studies by Fujita et al. [30], Piredda et al. [31], Ndengera et al. [32], and Schall et al. [33].
   - T_2 range of 40–2470 ms determined from T_2 mapping in healthy subjects [15] and a meta-analysis [3]
   - PD range of 59%–97% determined from studies by Hagiwara et al. [5], Gasparovic et al. [15], and Schall et al. [33].

3 | Results

Tissue fractions and data quality measures reported for each of the six voxels can be found in Table S1. No data were excluded due to data quality. The signal-to-noise ratio (SNR) was greater than 20 for all measures (mean = 40.83, sd = 6.66), and the full width at half maximum (FWHM) of each spectrum was less than 0.07 ppm (mean = 0.03 ppm, sd = 0.008 ppm).

Table 1 shows a summary of the measured parameters averaged over all voxels (anterior and posterior, GM, WM, and mixed). A summary of the parameters for each of the six voxels can be found in Table S1. Example T_1, T_2, and PD maps from a single participant can be seen in Figure 2.

Figure 3 shows the measured T_1, T_2, and PD values separated by region. A significant difference was seen between regions for T_1 WM ($\beta = -0.02$, $p < 0.001$) and CSF ($\beta = 0.58$, $p < 0.001$), T_2 for the full voxel ($\beta = -0.004$, $p = 0.05$), GM ($\beta = -0.003$, $p < 0.001$) and WM ($\beta = -0.002$, $p < 0.001$), and for PD in WM ($\beta = -0.009$, $p < 0.001$) and CSF ($\beta = 0.03$, $p < 0.001$) regions.

WM T_1 was significantly higher in females compared to males ($\beta = -0.02$, $p = 0.02$). There were no other significant differences between sexes. There was a significant negative relationship between GM PD and age ($\beta = -0.001$, $p = 0.008$). There were no other significant relations with age.

3.1 | Comparison of Neurochemical Concentrations Calculated With Literature vs. Measured Values

Table 2 shows the mean concentration in mmol/kg for each metabolite calculated using standard literature values for T_1, T_2, and PD (LIT), as well as the average of the individual measurements from the full voxel (FULL) and tissue specific (SEG) values. The difference comparisons are also shown.

TABLE 1 | Values of each parameter obtained from the literature and mean ± standard deviation of the values measured from individual participants.

	Literature values [reference numbers]	Measured values
T_1 Full (s)	n/a	1.25 ± 0.30
T_1 GM (s)	1.33 [10, 34–36]	1.47 ± 0.10
T_1 WM (s)	0.83 [10, 34–36]	0.85 ± 0.03
T_1 CSF (s)	3.82 [37, 38]	2.92 ± 0.52
T_2 Full (ms)	n/a	70 ± 10
T_2 GM (ms)	110 [10, 34, 35]	70 ± 3
T_2 WM (ms)	80 [10, 34, 35]	60 ± 3
T_2 CSF (ms)	500 [39–41]	140 ± 4
PD Full	n/a	0.78 ± 0.04
PD GM	0.65 [15]	0.84 ± 0.02
PD WM	0.78 [15]	0.71 ± 0.01
PD CSF	0.97 [15]	0.95 ± 0.09

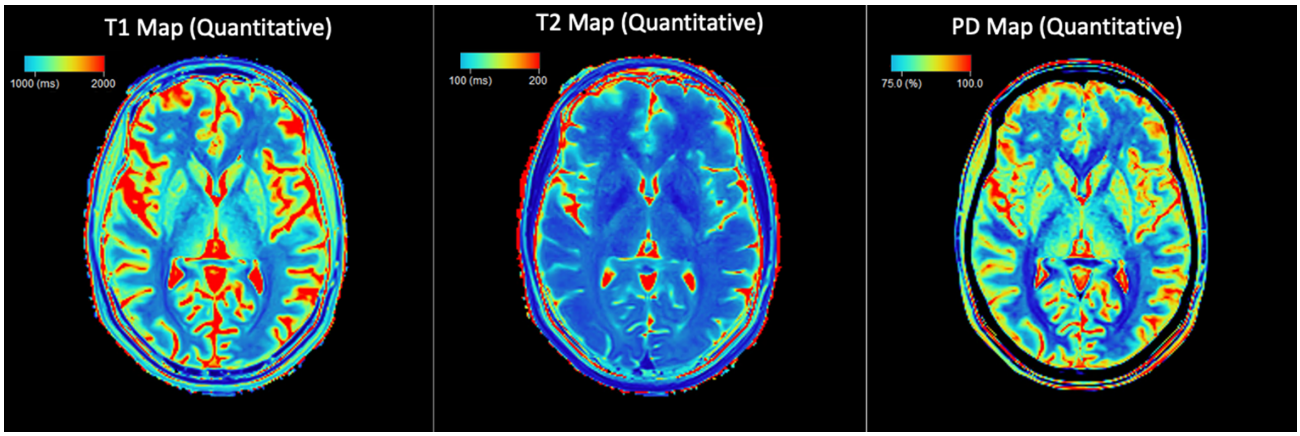

FIGURE 2 | Quantitative T_1, T_2, and PD maps from a single participant generated in SyMRI. These synthetic images depict the quantitative values of tissue relaxation times (T_1 and T_2) and PD.

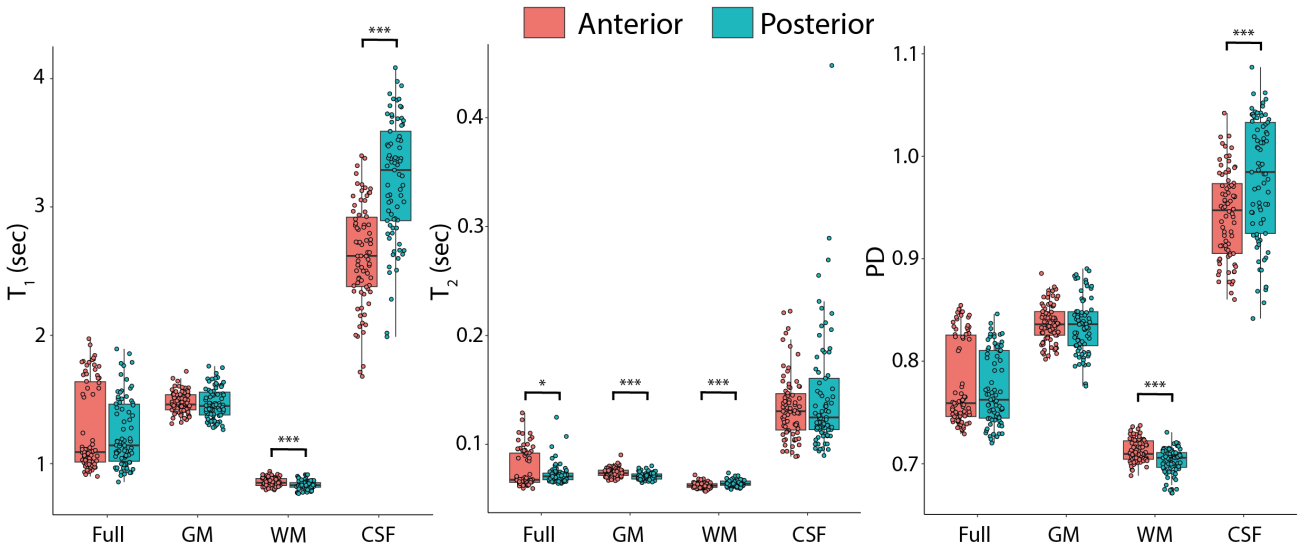

FIGURE 3 | Box plots showing median and interquartile range of T_1, T_2 and proton density (PD) values separated by region. Orange = anterior voxels, blue = posterior voxels. ***$p < 0.001$, *$p < 0.05$.

Figure 4 shows correlation and Bland–Altman plots for tNAA. Plots for the other neurochemicals are similar and can be found in the Supporting Information. All β estimates indicate a strong relationship between the literature and measured concentrations (regardless of whether FULL or SEG values were used). Metabolite concentrations were generally higher when using literature values compared to measured values, however the mean difference and range of the limits of agreement were generally small, with less than a 10% difference for all comparisons. Proportional biases were present in all comparisons, as the concentration increased, the difference between the two measures decreased. The high β estimates and small differences indicate good agreement between the metabolite concentrations calculated using both the literature and measured values.

3.2 | Sensitivity Analysis

For the comparison LIT versus SEG using tissue values observed in the present study, only f_{GM}, f_{WM}, f_{CSF}, and c_{raw} significantly contributed to the model. However, when including a larger range, the contribution from T_1 values for each tissue became significant, in addition to tissue fractions and c_{raw}. In contrast, for the comparison LIT versus FULL using values observed in the present study, T_1 and T_2 significantly contributed to the model in addition to f_{CSF} and c_{raw}. When using a larger range of values, T_1 remained a significant contributor and the contribution from PD became significant (in addition to f_{CSF} and c_{raw}). The contribution from T_2 was no longer significant (Figure 5).

4 | Discussion

In this study, we successfully used a multi-dynamic multi-echo (MDME) acquisition to acquire individually measured T_1, T_2, and PD values in ^{1}H-MRS voxels, and used these values for calculating neurochemical concentrations. We show good agreement between values calculated using literature and measured values in healthy young adults, both when using values obtained from a full voxel and a tissue segmented voxel. Sensitivity analyses

TABLE 2 | Concentrations of metabolite levels calculated with the different parameters, along with the β estimate and standard error from the linear model assessing the relationship between metabolite levels calculated with the literature values versus the measured values.

	Concentration			β estimate (±SE)		Mean difference (% *of Lit*) [limits of agreement]	
	Lit	Full	Seg	Lit vs. Full	Lit vs. Seg	Lit vs. Full	Lit vs. Seg
tNAA	9.56 ± 1.33	8.93 ± 1.74	8.77 ± 1.61	0.74 ± 0.01***	0.80 ± 0.01***	0.63 (7%) [−0.43, 1.69]	0.80 (8%) [−0.06, 1.65]
tCr	6.66 ± 1.46	6.25 ± 1.77	6.14 ± 1.66	0.81 ± 0.007***	0.87 ± 0.007***	0.41 (6%) [−0.32, 1.14]	0.53 (8%) [−0.03, 1.10]
tCho	1.47 ± 0.37	1.37 ± 0.39	1.34 ± 0.38	0.93 ± 0.02***	0.97 ± 0.02*	0.10 (7%) [−0.08, 0.29]	0.13 (9%) [−0.03, 0.28]
Myo	4.20 ± 0.99	3.94 ± 1.15	3.95 ± 1.16	0.82 ± 0.008***	0.81 ± 0.008***	0.26 (6%) [−0.21, 0.73]	0.26 (6%) [−0.21, 0.72]
Glu	7.11 ± 0.01	6.70 ± 2.42	6.58 ± 2.29	0.86 ± 0.006***	0.91 ± 0.006***	0.41 (6%) [−0.36, 1.19]	0.55 (8%) [−0.03, 1.12]
Glx	9.05 ± 2.71	8.53 ± 3.13	8.56 ± 3.13	0.86 ± 0.006***	0.86 ± 0.006***	0.52 (6%) [−0.47, 1.51]	0.51 (6%) [−0.46, 1.49]

Note: The mean difference is reported in molar units and, in round brackets, as a percentage of the molar concentration calculated with the literature values, along with the limits of agreement (square brackets) in molar values. LIT refers to concentrations calculated using literature values, FULL refers to concentrations calculated using individually measured values from a full voxel, and SEG refers to concentrations calculated using individually measured values from a segmented voxel. *** $p < 0.001$.

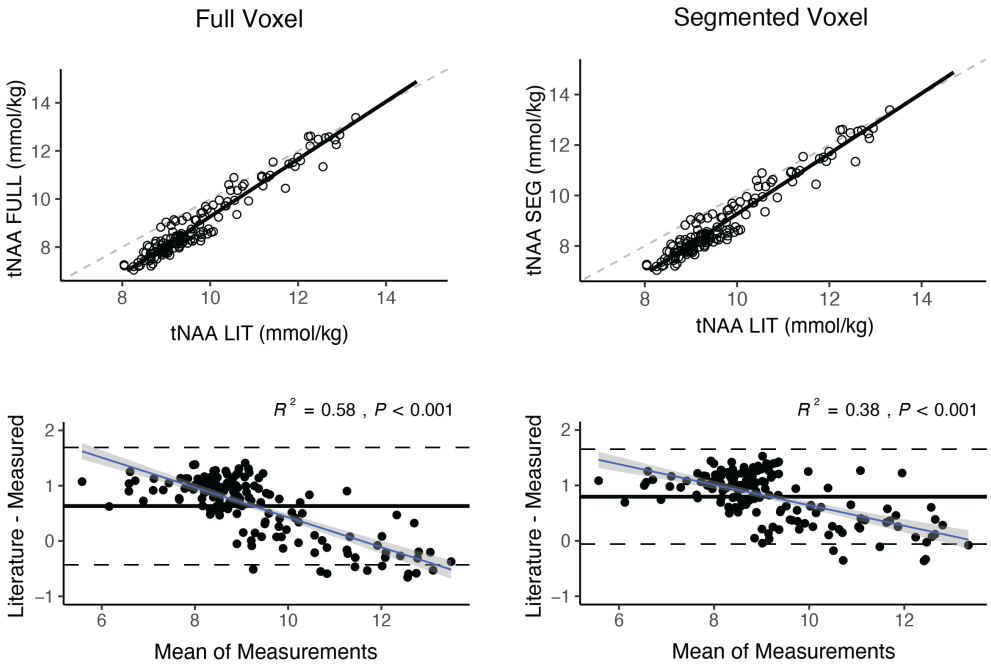

FIGURE 4 | Correlation and Bland–Alman plots for the comparison of tNAA calculated using the literature values (LIT) against tNAA calculated using the measured values. The left column contains values measured from the full voxel (FULL), and the right column contains values measured from the segmented voxel (SEG). The mean difference is indicated with the solid black line, and limits of agreement are indicated with dashed black lines. The blue line and gray shaded area indicate the linear relationship and 95% confidence of the two measures.

showed T_1 values to significantly contribute to metabolite concentration values, particularly when using a range larger than observed in the present population. This suggests in aging or clinical populations where T_1 may vary, individually measured T_1, T_2, and PD values may be beneficial to accurately interpret results.

Generally, the relaxation times in this study were similar to those seen in the literature, demonstrating the efficacy of using a MDME acquisition to acquire individually measured T_1, T_2, and PD values. This is highlighted by the strong agreement seen between metabolite concentrations calculated using both the literature and measured values. This strong agreement is likely due to the use of healthy young adults in this study, a similar population to those used in previous studies measuring these factors. Given the previous age relationships seen with these measures [4–9], it is expected that the relaxation times would

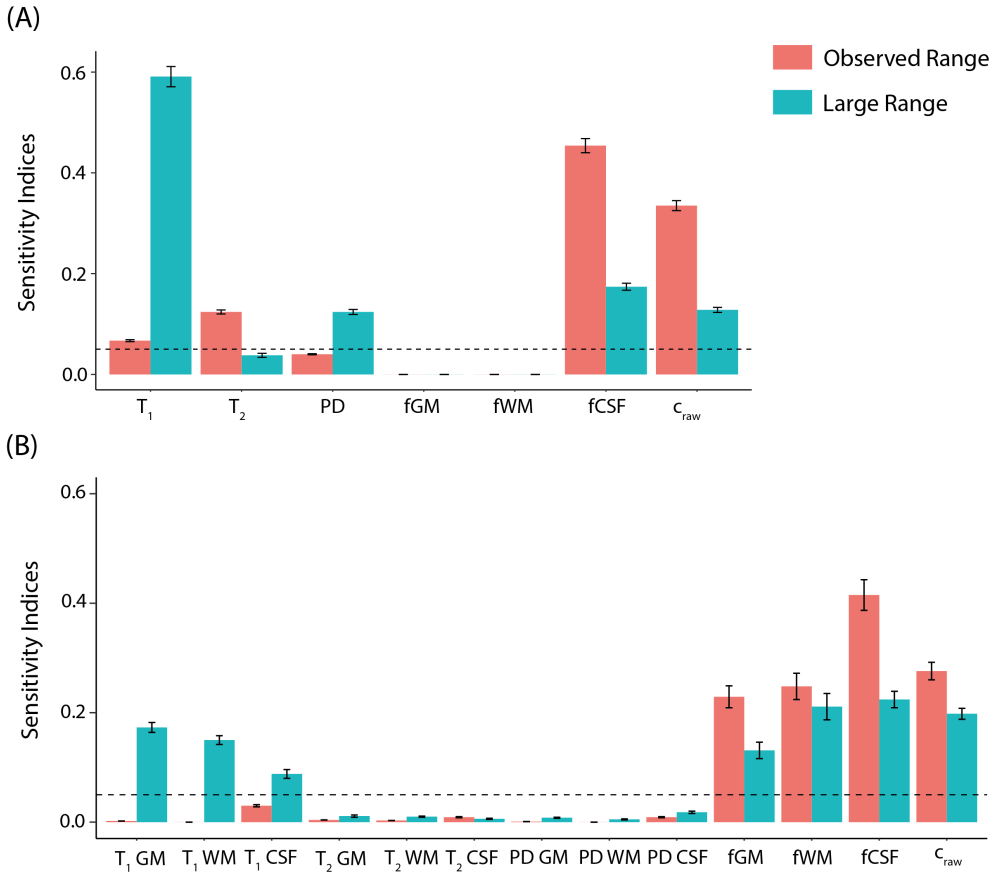

FIGURE 5 | (A) Sensitivity indices for each metric when using a full voxel. (B) Sensitivity indices for each metric when using a segmented voxel. Indices for tissue specific relaxation times and proton densities not shown in part (A) as they did not significantly contribute to the model, see Table 3 for values. Error bars represent 95% confidence intervals. Orange represents using data obtained from in vivo scans, blue represents using a larger range obtained from the literature. The dashed line indicates the cut-off value for statistical significance (0.05). Values larger than this were considered significant.

TABLE 3 | Input range and sensitivity indices with 95% CIs.

Metric	Input range		Full voxel		Segmented voxel	
	Observed	Large range	Observed range	Large range	Observed range	Large range
T_1 Full (s)	[0.857, 1.973]	[0.600, 6.873]	**0.067 ± 0.002**	**0.591 ± 0.020**	n/a	n/a
T_1 GM (s)	[1.265, 1.759]	[0.600, 6.873]	0.000 ± 0.000	0.000 ± 0.000	0.002 ± < 0.001	**0.173 ± 0.009**
T_1 WM (s)	[0.767, 0.940]	[0.600, 6.873]	0.000 ± 0.000	0.000 ± 0.000	< 0.001 ± < 0.001	**0.150 ± 0.008**
T_1 CSF (s)	[1.680, 4.085]	[0.600, 6.873]	0.000 ± 0.000	0.000 ± 0.000	0.030 ± 0.002	0.088 ± 0.008
T_2 Full (ms)	[59, 129]	[40, 2470]	**0.124 ± 0.004**	0.038 ± 0.004	n/a	n/a
T_2 GM (ms)	[65, 90]	[40, 2470]	0.000 ± 0.000	0.000 ± 0.000	0.004 ± < 0.001	0.011 ± 0.002
T_2 WM (ms)	[57, 74]	[40, 2470]	0.000 ± 0.000	0.000 ± 0.000	0.003 ± < 0.001	0.010 ± 0.001
T_2 CSF (ms)	[89, 448]	[40, 2470]	0.000 ± 0.000	0.000 ± 0.000	0.009 ± 0.001	0.006 ± 0.001
PD_{Full}	[0.720, 0.855]	[0.590, 0.970]	0.040 ± 0.001	**0.124 ± 0.005**	n/a	n/a
PD_{GM}	[0.776,0.890]	[0.590, 0.970]	< 0.001 ± 0.000	< 0.001 ± < 0.001	0.001 ± < 0.001	0.008 ± 0.001
PD_{WM}	[0.671,0.737]	[0.590, 0.970]	< 0.001 ± 0.000	< 0.001 ± 0.000	< 0.001 ± < 0.001	0.005 ± 0.001
PD_{CSF}	[0.842, 1.087]	[0.590, 0.970]	0.000 ± 0.000	0.000 ± 0.000	0.009 ± 0.001	0.018 ± 0.002
f_{GM}	[0.098, 0.912]	[0.098, 0.912]	0.000 ± 0.000	< 0.001 ± < 0.001	**0.229 ± 0.020**	**0.131 ± 0.015**
f_{WM}	[0.015, 0.896]	[0.015, 0.896]	0.000 ± 0.000	< 0.001 ± < 0.001	**0.248 ± 0.024**	**0.211 ± 0.024**
f_{CSF}	[0.001, 0.440]	[0.001, 0.440]	**0.454 ± 0.014**	**0.174 ± 0.007**	**0.415 ± 0.028**	**0.224 ± 0.015**
c_{raw}	[10.056, 16.729]	[10.056, 16.729]	**0.335 ± 0.010**	**0.128 ± 0.005**	**0.276 ± 0.016**	**0.198 ± 0.010**

Note: Sensitivity indices greater than 0.05 were interpreted to significantly contribute to the model and have been indicated in bold.

vary and subsequently the agreement between concentrations calculated with literature versus measured values would be weaker with values measured from older adults.

There were, however, some differences in relaxation times measured in the present study and literature values. T_1 and T_2 values for CSF were lower in the present study, and GM PD was higher in the present study compared to literature values. Relaxation factors for CSF have not been well studied, with a range reported in the few studies that have specifically measured CSF relaxation. This discrepancy is likely in part due to differences in the methods used, but region may also play a role. Using a T_2 preparation sequence, Spijkerman et al. [40] demonstrated CSF T_2 values were significantly shorter when measured in the periphery compared to the ventricles, and that partial volume effects lowered observed T_2 values. They hypothesize this is due to physiological differences between the areas, such as differences in oxygen, protein or glucose levels, which are known to decrease T_2. Similarly, Jiang et al. [42] used inversion recovery to demonstrate shorter T_1 and T_2 values in the subarachnoid space compared to the lateral ventricles. Additionally, T_1 and T_2 values decreased when moving in an anterior–posterior direction within the subarachnoid space. They postulate that the decreasing values relate to a faster brain-CSF water exchange rate, which was supported by evidence from simulations. These discrepancies highlight the need for individual and region-specific parameter measures, particularly for voxels with significant CSF partial volume effects.

To appropriately calculate metabolite concentrations, fractions of tissue within the voxel must be calculated, which is typically achieved by segmenting a T_1 structural scan. However, errors in segmentation will lead to errors in calculated concentrations, as evidenced by the substantial contribution of tissue fraction in our sensitivity analysis. Further, the slightly larger voxels in the MAGiC scans (1.24 mm^3) mean they will be more susceptible to segmentation errors. To investigate this, we extracted relaxation parameters from the whole voxel (FULL) and compared this to tissue segmented values (SEG). The mean difference between LIT versus SEG was slightly larger than that for LIT versus FULL, but both were of similar magnitude and all were below 10%. LIT versus FULL had slightly lower β estimates and a larger range for the limits of agreement for all metabolites except for Myo and Glx, where the range was similar for both comparisons, but again values were of a similar magnitude (e.g., LIT vs. FULL $\beta = 0.74$ vs. LIT vs. SEG $\beta = 0.80$ for tNAA). Due to a lack of ground truth, it is unknown which method is more accurate, however using values measured from the segmented voxel compared to the full voxel does not appear to have a large impact on the final values. Therefore, potential segmentation errors from the slightly different voxel sizes in the MDME acquisition has a negligible effect on metabolite concentrations, and researchers may choose to use measured values from the full voxel to remove an analysis step without compromising the quantification procedure. In addition to segmentation errors within the voxel, there may be minor biases at the voxel edge due to signal averaging across tissue boundaries, which may also potentially result in bias in the extracted relaxation values and the subsequent metabolite concentrations. However, given the large MRS voxel sizes, this will likely only account for a small proportion of the voxel (6% in this specific case) and will therefore likely only have a small effect on the resulting metabolite value. Using the FULL voxel mask would remove the impact of this on the extracted relaxation values, providing further support for this method.

In the case of the full voxel (FULL), the sensitivity analysis showed T_1 significantly contributes to the model in both cases (large range and observed range), although the contribution was substantially higher when using the large range. T_2 significantly contributed only with the observed range of values and PD significantly contributed only with a large range of values. In the case of the segmented voxel (SEG), T_1 significantly contributes to the model only when using a large range of values. T_2 and PD did not significantly contribute in either case. The strong contribution from T_1 and small contribution from T_2 are impacted by the TR and TE used in this study (3000 and 35 ms, respectively). It has been shown that TR can substantially influence metabolite concentrations reported due to T_1 effects and the incomplete signal recovery between acquisitions [43]. Studies have shown measured metabolite concentrations increase with increasing TR [44] with a larger effect seen on metabolites with longer T_1s [43]. To reduce these effects, a TR of approximately five times the length of the T_1 relaxation time is needed [44]. In the case of the T_1 of CSF using the values measured from this study (2.92 s), a TR over 14 s would be needed to remove T_1 effects, which would be prohibitive. However, a TR of 4.5 s results in a roughly 10% loss of signal without being prohibitively long [44], and may therefore reduce the impact of variation in T_1 values on quantification. In contrast, a short TE of 35 ms, which is lower than both the literature and measured water T_2 values, results in minimal T_2 decay [45] which may be why T_2 was shown to have a less significant contribution.

It should be noted that we did not perform a systematic review of the literature to determine our range of values for the sensitivity analysis. Where possible, we extracted the maximum and minimum values from reviews [2, 3]. Given that relaxation values depend strongly on the method used, including values obtained from multiple methods potentially creates more variation than is truly present; however, an overly restrictive range limits the utility of this sensitivity analysis. As a result, we chose to keep our values broad in an attempt to encompass results from many scenarios, but this large variation may over-inflate the contribution of parameters in the sensitivity analysis. As some parameters significantly (or nearly significantly) contributed in the case of both a small and a large range, we can confidently say these parameters significantly contribute to metabolite quantification and should be appropriately accounted for where possible.

Previously, multiple sequences were needed to individually measure relaxation factors and PD values. Gasparovic et al. [15] used T_1 mapping (TAPIR sequence), T_2 mapping (multiple spin echo sequence) and T_2* mapping (PD, QUTE sequence) to measure the three factors, requiring a substantial amount of scan time. Although MRS quantification was improved using this method, this is particularly burdensome to populations who are unable to stay in the scanner for long periods of time, typical of many clinical conditions. Additionally, studies including multiple MRI measures likely already have long protocols without space for multiple scans to acquire relaxation factors. Similar to the present study, Tisell et al. [46] demonstrated successful acquisition of MDME data (QRAPMASTER) on a Philips Achieva 1.5 T scanner to measure all three factors in a single scan, significantly reducing

the time burden. Here we expand on this work to show successful acquisition of individual relaxation parameters for MRS quantification using a MAGiC acquisition on a 3 T GE 750 W scanner. Similar to QRAPMASTER, MAGiC is a MDME sequence used for quantitative imaging on GE scanners, alternatively known as SyMRI on Philips and Siemens scanners. In addition to showing the feasibility of this sequence, we show that tissue segmentation can be performed on MDME data, allowing for correction of tissue specific relaxation in mixed-tissue voxels. This expands on the work by Tisell et al. [46], who used a primarily gray matter and primarily white matter voxel only. We also show that tissue segmentation is not a required step when using individually measured parameters, and relaxation factors comprising the mixed tissues can be used without loss of accuracy.

An alternative approach that falls between collecting individual relaxation values and using global literature values is to use literature values that are region and age specific. Simegn et al. [42] recently published an open access atlas to facilitate correction of region and age-related differences in T_1 and T_2 relaxation values. They collected relaxation values across the whole brain from participants aged 20–60 using DESPOT (Philips) and have provided these in a format where users can align their voxels to determine region specific values. While this is a useful resource, individual differences in T_1 and T_2 relaxation values across participants will not be accounted for, which may create variation in quantified metabolite values and may be particularly relevant in clinical studies. Additionally, PD is not included in these maps, which may contribute to variation in some cases, as shown in our sensitivity analysis. Errors from segmentation are also likely to be a greater issue with this method, given the need to adjust the data to fit an atlas. While both methods are a solution to a common problem in MRS quantification, the atlas is best suited to studies involving typical populations and is a potential compromise where the means to collect data for individually measured parameters is not available or restricted. However, researchers should be mindful of the limitations of this atlas. Alternatively, we have demonstrated collection of individual parameters is possible in a short time period, and may be particularly relevant in clinical or pediatric populations where relaxation values will likely vary from the atlas. In this study we collected all three parameters in under 5 min, making it possible to add this scan to a session without adding substantial time burden.

A limitation of this proof-of-concept demonstration study is the use of a healthy young population for measuring relaxation factors, reducing the variability. Although we did find a relationship between age and GM PD, other age relationships reported in the literature [4–9] were not seen in this sample, likely due to the narrow age range. To make our findings more applicable to other populations, we included a larger range of values obtained from the literature in our sensitivity analysis. However, we did not conduct a systematic review of the literature and therefore it is possible that studies will include parameters outside of this range. We recommend studies using populations where T_1, T_2 and PD may vary to obtain individually measured factors, particularly for T_1 if using similar acquisition parameters to the present study. The use of MDME acquisitions means the time burden of adding this measurement to a MRI session is low, making it more accessible to researchers, particularly those working with populations who are unable to remain in the MRI scanner for long periods of time.

5 | Conclusion

In conclusion, we show feasibility of using a multi-contrast acquisition to acquire individually measured T_1, T_2, and PD values for neurochemical signal correction in ^{1}H-MRS. We found good agreement with concentrations calculated using literature values and individually observed values in healthy young adults. However, sensitivity analyses highlighted the necessity of measuring these parameters in atypical populations where the parameters are likely to vary beyond those typically reported, or where the parameters themselves may be related to the measure of interest.

Acknowledgments

The authors acknowledge the technical and scientific contributions of Dr. Louis Lauzon (University of Calgary) to this study. Additional support was provided by the Hotchkiss Brain Institute and the Alberta Children's Hospital Research Institute.

Funding

This work was supported by funding from the Natural Sciences and Engineering Research Council of Canada (NSERC Discovery Grant to A.D.H.) as well as a CFI-JELF award to A.D.H. A.D.H. also hold a Canada Research Chair in Magnetic Resonance Spectroscopy in Brain Injury and Pain. S.A.L. was supported by the Natural Sciences and Engineering Research Council of Canada (NSERC) Canada Graduate Scholarships — Doctoral (CGS D) program.

Data Availability Statement

The data that support the findings of this study are available from the corresponding author upon reasonable request.

References

1. J. Near, A. D. Harris, C. Juchem, et al., "Preprocessing, Analysis and Quantification in Single-Voxel Magnetic Resonance Spectroscopy: Experts' Consensus Recommendations," *NMR in Biomedicine* 34 (2020): e4257, https://doi.org/10.1002/nbm.4257.

2. J. Z. Bojorquez, S. Bricq, C. Acquitter, F. Brunotte, P. M. Walker, and A. Lalande, "What Are Normal Relaxation Times of Tissues at 3 T?," *Magnetic Resonance Imaging* 35 (2017): 69–80, https://doi.org/10.1016/j.mri.2016.08.021.

3. A. T. Gudmundson, A. Koo, A. Virovka, et al., "Meta-Analysis and Open-Source Database for In Vivo Brain Magnetic Resonance Spectroscopy in Health and Disease," *Analytical Biochemistry* 676 (2023): 676, https://doi.org/10.1016/j.ab.2023.115227.

4. L. Nürnberger, R.-M. Gracien, P. Hok, et al., "Longitudinal Changes of Cortical Microstructure in Parkinson's Disease Assessed With T1 Relaxometry," *NeuroImage Clinical* 13 (2017): 405–414, https://doi.org/10.1016/j.nicl.2016.12.025.

5. A. Hagiwara, K. Fujimoto, K. Kamagata, et al., "Age-Related Changes in Relaxation Times, Proton Density, Myelin, and Tissue Volumes in Adult Brain Analyzed by 2-Dimensional Quantitative Synthetic Magnetic Resonance Imaging," *Investigative Radiology* 56 (2021): 163–172, https://doi.org/10.1097/RLI.0000000000000720.

6. R. Kumar, S. Delshad, M. A. Woo, P. M. Macey, and R. M. Harper, "Age-Related Regional Brain T2-Relaxation Changes in Healthy Adults," *Journal of Magnetic Resonance Imaging* 35 (2012): 300–308, https://doi.org/10.1002/jmri.22831.

7. R. Kumar, S. Delshad, P. M. Macey, M. A. Woo, and R. M. Harper, "Development of T2-Relaxation Values in Regional Brain Sites During

Adolescence," *Magnetic Resonance Imaging* 29 (2011): 185–193, https://doi.org/10.1016/j.mri.2010.08.006.

8. E. J. Canales-Rodríguez, S. Alonso-Lana, N. Verdolini, et al., "Age- and Gender-Related Differences in Brain Tissue Microstructure Revealed by Multi-Component T2 Relaxometry," *Neurobiology of Aging* 106 (2021): 68–79, https://doi.org/10.1016/j.neurobiolaging.2021.06.002.

9. M. J. Knight, B. McCann, D. Tsivos, S. Dillon, E. Coulthard, and R. A. Kauppinen, "Quantitative T2 Mapping of White Matter: Applications for Ageing and Cognitive Decline," *Physics in Medicine and Biology* 61 (2016): 5587–5605, https://doi.org/10.1088/0031-9155/61/15/5587.

10. J. Vymazal, A. Righini, R. A. Brooks, et al., "T1 and T2 in the Brain of Healthy Subjects, Patients With Parkinson Disease, and Patients With Multiple System Atrophy: Relation to Iron Content," *Radiology* 211 (1999): 489–495, https://doi.org/10.1148/radiology.211.2.r99ma53489.

11. N. Gelman, J. M. Gorell, P. B. Barker, et al., "MR Imaging of Human Brain at 3.0 T: Preliminary Report on Transverse Relaxation Rates and Relation to Estimated Iron Content," *Radiology* 210 (1999): 759–767, https://doi.org/10.1148/radiology.210.3.r99fe41759.

12. R.-M. Gracien, L. Nürnberger, P. Hok, et al., "Evaluation of Brain Ageing: A Quantitative Longitudinal MRI Study Over 7 Years," *European Radiology* 27 (2017): 1568–1576, https://doi.org/10.1007/s00330-016-4485-1.

13. A. R. Wearn, V. Nurdal, E. Saunders-Jennings, et al., "T2 Heterogeneity: A Novel Marker of Microstructural Integrity Associated With Cognitive Decline in People With Mild Cognitive Impairment," *Alzheimer's Research & Therapy* 12 (2020): 105, https://doi.org/10.1186/s13195-020-00672-9.

14. L. Sporn, E. L. MacMillan, R. Ge, K. Greenway, F. Vila-Rodriguez, and C. Laule, "Longer Repetition Time Proton MR Spectroscopy Shows Increasing Hippocampal and Parahippocampal Metabolite Concentrations With Aging," *Journal of Neuroimaging* 29 (2019): 592–597, https://doi.org/10.1111/jon.12648.

15. C. Gasparovic, H. Neeb, D. L. Feis, et al., "Quantitative Spectroscopic Imaging With in Situ Measurements of Tissue Water T1, T2, and Density," *Magnetic Resonance in Medicine* 62 (2009): 583–590, https://doi.org/10.1002/mrm.22060.

16. L. N. Tanenbaum, A. J. Tsiouris, A. N. Johnson, et al., "Synthetic MRI for Clinical Neuroimaging: Results of the Magnetic Resonance Image Compilation (MAGiC) Prospective, Multicenter, Multireader Trial," *American Journal of Neuroradiology* 38 (2017): 1103–1110, https://doi.org/10.3174/ajnr.A5227.

17. L. Nunez-Gonzalez, K. A. van Garderen, M. Smits, et al., "Pre-Contrast MAGiC in Treated Gliomas: A Pilot Study of Quantitative MRI," *Scientific Reports* 12 (2022): 21820, https://doi.org/10.1038/s41598-022-24276-5.

18. J. B. M. Warntjes, O. Dahlqvist Leinhard, J. West, and P. Lundberg, "Rapid Magnetic Resonance Quantification on the Brain: Optimization for Clinical Usage," *Magnetic Resonance in Medicine* 60 (2008): 320–329, https://doi.org/10.1002/mrm.21635.

19. J. B. M. Warntjes, O. Dahlqvist, and P. Lundberg, "Novel Method for Rapid, Simultaneous T_1, T_2, and Proton Density Quantification," *Magnetic Resonance in Medicine* 57 (2007): 528–537, https://doi.org/10.1002/mrm.21165.

20. SyntheticMR AB, "SyMRI SyntheticMR AB User Manual," 2021.

21. A. Hagiwara, M. Warntjes, M. Hori, et al., "SyMRI of the Brain," *Investigative Radiology* 52 (2017): 647–657, https://doi.org/10.1097/RLI.0000000000000365.

22. R. Simpson, G. A. Devenyi, P. Jezzard, T. J. Hennessy, and J. Near, "Advanced Processing and Simulation of MRS Data Using the FID Appliance (FID-A)—An Open Source, MATLAB-Based Toolkit," *Magnetic Resonance in Medicine* 77 (2017): 23–33, https://doi.org/10.1002/mrm.26091.

23. S. W. Provencher, "Estimation of Metabolite Concentrations From Localized In Vivo Proton NMR Spectra," *Magnetic Resonance in Medicine* 30 (1993): 672–679, https://doi.org/10.1002/mrm.1910300604.

24. A. D. Harris, N. A. J. Puts, and R. A. E. Edden, "Tissue Correction for GABA-Edited MRS: Considerations of Voxel Composition, Tissue Segmentation, and Tissue Relaxations," *Journal of Magnetic Resonance Imaging* 42 (2015): 1431–1440, https://doi.org/10.1002/jmri.24903.

25. M. Jenkinson, C. F. Beckmann, T. E. Behrens, M. W. Woolrich, and S. M. Smith, "FSL," *NeuroImage* 62 (2012): 782–790.

26. R Core Team, *R: A Language and Environment for Statistical Computing* (R Foundation for Statistical Computing, 2020), https://www.R-project.org/.

27. D. Bates, M. Mächler, B. Bolker, and S. Walker, "Fitting Linear Mixed-Effects Models Using lme4," *Journal of Statistical Software* 1 (2015): 1–48, https://doi.org/10.18637/jss.v067.i01.

28. X. Zhang, M. Trame, L. Lesko, and S. Schmidt, "Sobol Sensitivity Analysis: A Tool to Guide the Development and Evaluation of Systems Pharmacology Models," *CPT: Pharmacometrics & Systems Pharmacology* 4 (2015): 69–79, https://doi.org/10.1002/psp4.6.

29. C. Gasparovic, H. Chen, and P. G. Mullins, "Errors in 1 H-MRS Estimates of Brain Metabolite Concentrations Caused by Failing to Take Into Account Tissue-Specific Signal Relaxation," *NMR in Biomedicine* 31 (2018): e3914, https://doi.org/10.1002/nbm.3914.

30. S. Fujita, A. Hagiwara, K. Kimura, et al., "Three-Dimensional Simultaneous T1 and T2* Relaxation Times and Quantitative Susceptibility Mapping at 3 T: A Multicenter Validation Study," *Magnetic Resonance Imaging* 112 (2024): 100–106, https://doi.org/10.1016/j.mri.2024.07.004.

31. G. F. Piredda, T. Hilbert, C. Granziera, et al., "Quantitative Brain Relaxation Atlases for Personalized Detection and Characterization of Brain Pathology," *Magnetic Resonance in Medicine* 83 (2020): 337–351, https://doi.org/10.1002/mrm.27927.

32. M. Ndengera, B. M. A. Delattre, M. Scheffler, K. O. Lövblad, T. R. Meling, and M. I. Vargas, "Relaxation Time of Brain Tissue in the Elderly Assessed by Synthetic MRI," *Brain and Behavior* 12 (2022): 1–9, https://doi.org/10.1002/brb3.2449.

33. M. Schall, M. Zimmermann, E. Iordanishvili, Y. Gu, N. Jon Shah, and A. M. Oros-Peusquens, "A 3D Two-Point Method for Whole-Brain Water Content and Relaxation Time Mapping: Comparison With Gold Standard Methods," *PLoS One* 13 (2018): 1–21, https://doi.org/10.1371/journal.pone.0201013.

34. J. P. Wansapura, S. K. Holland, R. S. Dunn, and W. S. Ball, "NMR Relaxation Times in the Human Brain at 3.0 Tesla," *Journal of Magnetic Resonance Imaging* 9 (1999): 531–538, https://doi.org/10.1002/(SICI)1522-2586(199904)9:4<531::AID-JMRI4>3.0.CO;2-L.

35. G. J. Stanisz, E. E. Odrobina, J. Pun, et al., "T1, T2 Relaxation and Magnetization Transfer in Tissue at 3T," *Magnetic Resonance in Medicine* 54 (2005): 507–512, https://doi.org/10.1002/mrm.20605.

36. T. Ethofer, I. Mader, U. Seeger, et al., "Comparison of Longitudinal Metabolite Relaxation Times in Different Regions of the Human Brain at 1.5 and 3 Tesla," *Magnetic Resonance in Medicine* 50 (2003): 1296–1301, https://doi.org/10.1002/mrm.10640.

37. H. Lu, L. M. Nagae-Poetscher, X. Golay, D. Lin, M. Pomper, and P. C. M. Van Zijl, "Routine Clinical Brain MRI Sequences for Use at 3.0 Tesla," *Journal of Magnetic Resonance Imaging* 22 (2005): 13–22, https://doi.org/10.1002/jmri.20356.

38. W. D. Rooney, G. Johnson, X. Li, et al., "Magnetic Field and Tissue Dependencies of Human Brain Longitudinal ^1H_2O Relaxation In Vivo," *Magnetic Resonance in Medicine* 57 (2007): 308–318, https://doi.org/10.1002/mrm.21122.

39. S. K. Piechnik, J. Evans, L. H. Bary, R. G. Wise, and P. Jezzard, "Functional Changes in CSF Volume Estimated Using Measurement of Water

T2 Relaxation," *Magnetic Resonance in Medicine* 61 (2009): 579–586, https://doi.org/10.1002/mrm.21897.

40. J. M. Spijkerman, E. T. Petersen, J. Hendrikse, P. Luijten, and J. J. M. Zwanenburg, "T 2 Mapping of Cerebrospinal Fluid: 3 T Versus 7 T," *Magnetic Resonance Materials in Physics, Biology and Medicine* 31 (2018): 415–424, https://doi.org/10.1007/s10334-017-0659-3.

41. C. Gasparovic, R. Yeo, M. Mannell, et al., "Neurometabolite Concentrations in Gray and White Matter in Mild Traumatic Brain Injury: An ^{1}H-Magnetic Resonance Spectroscopy Study," *Journal of Neurotrauma* 26 (2009): 1635–1643, https://doi.org/10.1089/neu.2009.0896.

42. D. Jiang, Y. Gou, Z. Wei, X. Hou, V. Yedavalli, and H. Lu, "Quantification of T_1 and T_2 of Subarachnoid CSF: Implications for Water Exchange Between CSF and Brain Tissues," *Magnetic Resonance in Medicine* 90 (2023): 2411–2419, https://doi.org/10.1002/mrm.29829.

43. A. G. Ensworth, L. R. Barlow, P. Kozlowski, E. L. MacMillan, and C. Laule, "The Goldilocks Zone for 3-T MRS Studies Using Semi-LASER: Determining the Optimal Balance Between Repetition Time and Scan Time," *NMR in Biomedicine* 38 (2025): 1–10, https://doi.org/10.1002/nbm.70064.

44. J. Knight-Scott, P. Brennan, S. Palasis, and X. Zhong, "Effect of Repetition Time on Metabolite Quantification in the Human Brain in 1H MR Spectroscopy at 3 Tesla," *Journal of Magnetic Resonance Imaging* 45 (2017): 710–721, https://doi.org/10.1002/jmri.25403.

45. M. Wilson, O. Andronesi, P. B. Barker, et al., "Methodological Consensus on Clinical Proton MRS of the Brain: Review and Recommendations," *Magnetic Resonance in Medicine* 82 (2019): 527–550, https://doi.org/10.1002/mrm.27742.

46. A. Tisell, O. D. Leinhard, J. B. M. Warntjes, and P. Lundberg, "Procedure for Quantitative 1H Magnetic Resonance Spectroscopy and Tissue Characterization of Human Brain Tissue Based on the Use of Quantitative Magnetic Resonance Imaging," *Magnetic Resonance in Medicine* 70 (2013): 905–915, https://doi.org/10.1002/mrm.24554.

Supporting Information

Additional supporting information can be found online in the Supporting Information section. **Figure S1:** Correlation and Bland–Alman plots for the comparison of tCr calculated using the literature values against tCr calculated using the measured values. The left column contains values measured from the full voxel, and the right column contains values measured from the segmented voxel. The mean difference is indicated with the solid black line, and limits of agreement are indicated with dashed black lines. The blue line and gray shaded area indicate the linear relationship and 95% confidence of the two measures. **Figure S2:** Correlation and Bland–Alman plots for the comparison of tCho calculated using the literature values against tCho calculated using the measured values. The left column contains values measured from the full voxel, and the right column contains values measured from the segmented voxel. The mean difference is indicated with the solid black line, and limits of agreement are indicated with dashed black lines. The blue line and gray shaded area indicate the linear relationship and 95% confidence of the two measures. **Figure S3:** Correlation and Bland–Alman plots for the comparison of Myo calculated using the literature values against Myo calculated using the measured values. The left column contains values measured from the full voxel, and the right column contains values measured from the segmented voxel. The mean difference is indicated with the solid black line, and limits of agreement are indicated with dashed black lines. The blue line and gray shaded area indicate the linear relationship and 95% confidence of the two measures. **Figure S4:** Correlation and Bland–Alman plots for the comparison of Glu calculated using the literature values against Glu calculated using the measured values. The left column contains values measured from the full voxel, and the right column contains values measured from the segmented voxel. The mean difference is indicated with the solid black line, and limits of agreement are indicated with dashed black lines. The blue line and gray shaded area indicate the linear relationship and 95% confidence of the two measures. **Figure S5:** Correlation and Bland–Alman plots for the comparison of Glx calculated using the literature values against Glx calculated using the measured values. The left column contains values measured from the full voxel, and the right column contains values measured from the segmented voxel. The mean difference is indicated with the solid black line, and limits of agreement are indicated with dashed black lines. The blue line and gray shaded area indicate the linear relationship and 95% confidence of the two measures. **Table S1:** Mean ± standard deviation of quality metrics, tissue fraction and multi-contrast acquisition parameters separated by voxel composition and location. **Table S2:** Metabolite relaxation values by tissue.